IEEE Access
Multidisciplinary ⋮ Rapid Review ⋮ Open Access Journal

Received October 14, 2020, accepted October 22, 2020, date of publication October 26, 2020, date of current version November 6, 2020.

Digital Object Identifier 10.1109/ACCESS.2020.3033894

PARDOS: An Educational Software Tool for the Analysis of Sound Propagation

DOMINGO PARDO-QUILES[1], JOSÉ-VÍCTOR RODRÍGUEZ[1], AND IGNACIO RODRÍGUEZ-RODRÍGUEZ[2]

[1]Departamento de Tecnologías de la Información y las Comunicaciones, Universidad Politécnica de Cartagena, 30202 Cartagena, Spain
[2]Departamento de Ingeniería de Comunicaciones, ATIC Research Group, Universidad de Málaga, 29071 Málaga, Spain

Corresponding author: José-Víctor Rodríguez (jvictor.rodriguez@upct.es)

This work was supported in part by the Ministerio de Ciencia e Innovación, Spain, under Grant TEC2016-78028-C3-2-P and Grant PID2019-107885GB-C33/AEI/10.13039/501100011033, and in part by the European Fonds Européen de Développement Économique et Régional (FEDER) Funds. The work of Ignacio Rodríguez-Rodríguez was supported in part by the Programa Operativo FEDER Andalucía 2014–2020 under Project UMA18-FEDERJA-023, and in part by the Universidad de Málaga, Campus de Excelencia Internacional Andalucía Tech.

ABSTRACT The educational software tool PARDOS is presented for the analysis of sound propagation, being applicable for supplementing and enhancing the understanding and learning of the principles of acoustic engineering thanks to the features it offers. With this tool, students (high school or undergraduate as well as Ph.D.) will be able to create environments – multi-modeled obstacles – and settings based on real scenarios, load acoustic sources, simulate the expected insertion losses (IL) and acoustic attenuation at any receiver (listener) location, or use the auralization module to test the acoustic quality of the design carried out. Moreover, the learning of the fundamentals of acoustic propagation is supported by a set of four guided practices embedded in the software application, which can also be very useful for teachers. The main advantage of the presented tool is that, unlike most of the computationally demanding alternatives for acoustic propagation – which usually imply complex CAD files, and highly dense raytracing approaches – PARDOS is a user-friendly teaching-oriented software developed with MATLAB that successfully combines the use of the Uniform Theory of Diffraction (UTD), Image Source (IS) method, graph theory, funicular polygons, and Fresnel ellipsoids to obtain high accuracy performances while significantly lowering computational requirements. Moreover, the design of any obstacle can easily be achieved using the proper combination of wedges, rectangles, cylinders, and T/Y-shaped structures.

INDEX TERMS Educational software, engineering education, acoustic propagation, multiple sound diffraction, uniform theory of diffraction.

I. INTRODUCTION

Acoustic engineering is a multidisciplinary branch encompassing many aspects of modern society. Many different fields require high demands from the profession, for example: architectural acoustics (acoustic insulation and conditioning, e.g. for creating better-sounding concert halls); environmental acoustics (noise maps, outdoor industrial noise, vehicle noise), electroacoustics; materials characterization; facilities (air conditioning and machinery); safety and hygiene at work in relation to noise protection; aerial and underwater acoustics (location of objects, communication, and sonar), etc. Teaching the principles of Acoustics may be of great interest, therefore, at high school and undergraduate educational levels, while being essential for university degrees such as industrial/civil engineering or architecture.

Several computer-aided tools exist for the simulation of room acoustics based mostly on either wave-theoretical or Geometric Acoustics (GA) approaches. GA methods can be briefly classified within three main 'branches' ([1], [2]): Reflection *path-based* GA techniques, where the final signal response is calculated by properly combining the contributions of all selected reflected or diffracted paths; *surface-based* GA models, where surfaces act as an intermediate storage of acoustic energy (the sound energy is propagated from the source to the surrounding surfaces, and then further

The associate editor coordinating the review of this manuscript and approving it for publication was Martin Reisslein.

propagates along surfaces up to the receiver); and *hybrid* approaches combining path- and surface-based techniques.

Path-based GA techniques in acoustic computation can subsequently be classified into three main widely used models: Image Source (IS) methods, ray tracing, and beam tracing techniques. An extension incorporating diffraction modeling is also possible in any of these three path-based GA approaches.

The IS method is a path-based method that ideally models specular reflections by taking virtual sources into account [3]. They are constructed with a mirroring location of the initial source with respect to the relevant surfaces of the environment. It can be used in hybrid models and combined with tracing, diffracting or GA surface techniques.

Ray tracing is a very well-known and simple implementation technique [4] wherein the sound signal is emitted by a source through a finite number of rays with a homogeneous random distribution; for this reason, it can be subject to sampling errors (aliasing). Another widely used technique in acoustic computation is the beam tracing method, which overcomes the aliasing problem by recursively tracing beams (bundles of rays) with different cross-sections (e.g. cone, rectangular or frustum tracing) [5]; however, it can present some difficulties dealing with curved surfaces and refractions. The stochastic nature of tracing techniques means that no exact same response will be obtained from one simulation to the next, even when the setting parameters have not changed. In contrast, IS methods are deterministic.

Radiosity methods [6] or Acoustic Radiance Transfer (ART) techniques [7] should also be highlighted within surface-based GA modeling. However, both room geometrical constraints and computation complexity remain an issue in the former, and computation time and storage usage are still high for the latter. Moreover, ART is unable to accurately include edge diffraction. Therefore, these methods currently do not seem practical for large environments.

In stark contrast to the GA models, the wave-based methods deal with the numerical solution of the wave equation. The numerical methods are mainly classified within the Finite Difference Time Domain (FDTD) techniques [8], the Finite Element Methods (FEM) [9] and the Boundary Element Methods (BEM) [10]. These methods mesh the domain into small elements such that the differential wave equation can be more easily solved. Since the elements must be smaller than the shortest wavelength, the computation costs typically increase as the third power of the frequency; hence, these methods are restricted to low frequencies.

On the other hand, all the mentioned GA models typically exhibit high inaccuracies for wavelengths of the order of magnitude of the dimensions of the scenario under study (lowest frequencies) as diffraction and interference cannot be neglected at such frequencies. However, they are much faster and more reliable at higher frequencies than the wave methods. Moreover, most acousticians emphasize that accurate results ground in the quality of the input data. It is essential to guarantee an exact match of the real situation with the input parameters of the numerical model, encompassing the geometric model of the acoustic scene, the behavior of the sources and receivers, and the acoustic boundary conditions. Many experts still agree on the need to also rely on wave models for lower frequencies. The future of acoustics simulation and auralization tools offers potential improvement in predicting the perceptual properties of sound sources in virtual acoustic environments, enhanced development and relevance of dynamic simulations for virtual acoustic reality, and the exploitation of programmable graphics hardware to accelerate simulation calculations.

For these reasons and trade-offs, many software packages for outdoor and indoor acoustical modeling implement path-based GA, primarily through the use of ray tracing together with the IS method (for the efficient handling of low-order specular reflections). This is the case with several well-known professional software tools– such as CATT-Acoustic [11], EASE [12], RAYNOISE [13], COMSOL [14] or ODEON [15] – which feature an extended range of modules and capabilities that can surely fulfill the needs of professional acoustic engineers. Overall, the diffraction phenomenon is not managed by classical GA methods. However, diffraction modeling has lately been incorporated into some of the abovementioned popular commercial GA implementations, such as CATT and ODEON [16].

These software tools have significantly varying capabilities and exhibit different computational performances. However, the license rights to work with such professional tools within the educational field are not affordable for some schools/universities and their free demo versions are typically limited to a short time period or else to a highly constrained performance. Moreover, the calculations carried out within this professional software usually imply complex CAD files, and highly dense raytracing approaches, making them very computationally demanding and exceeding the performance of the laboratory computers available in most schools/universities and the time planned for a laboratory session. Furthermore, some of the most recent geometric acoustic implementations require the support of extra computer graphics hardware to increase the simulation efficiency [17].

As to the best of the authors' knowledge, a few software tools developed by academic institutions exist, albeit not for educational purposes. Examples include RAVEN (Room Acoustics for Virtual Environments), which is a hybrid algorithm that uses image sources for the direct sound and early reflections as well as ray tracing for the late reverberation [18]; RAZR (Room Acoustic Simulator) [19], which simulates rectangular rooms through a combination of image sources and a feedback delay network for late reverberation; and BRASS (Brazilian Room Acoustic Simulation Software) [20], which groups reflections up to the fifth order without deploying an image source model. In any case, the aforementioned shortcomings of the professional tools still exist in these tools when it comes to their application in educational contexts.

Therefore, regarding the above, there is no specific educational software focused on assisting student learning of acoustic propagation, diffraction and reflection phenomena.

In this respect, the motivation of this work is presenting the educational software PARDOS (acronym from Spanish 'Pérdidas Acústicas por Reflexión y Difracción de las Ondas Sonoras', which means '*Acoustic Losses due to the Reflection and Diffraction of Sound Waves*') – a new tool developed in MATLAB [21] from MathWorks that can be used within science (Physics, Maths) or engineering studies. Thus, the goal is to support students to learn about (and become familiar with) Acoustics via a user-friendly computer environment with the aim of preparing them to enter the job market (PARDOS has been programmed using the Graphical User Interface [GUI], provided by the Guide package of MATLAB in order to offer a more friendly and intuitive interface). The main advantage of the presented tool is that, unlike most computationally demanding professional tools for acoustic propagation, PARDOS successfully combines the use of the IS method and the Uniform Theory of Diffraction (UTD) with graph theory, funicular polygons, and Fresnel ellipsoids to obtain a high accuracy while significantly lowering the computational requirements [22]. In this respect, PARDOS can consider arbitrary reflection and edge diffraction events in any order to obtain the attenuation or insertion losses (IL) with very low memory usage and computation times in contrast to many professional or educational software tools [1].

It should be noted that one of the common misconceptions surrounding the abovementioned professional GA software packages is that such tools require very little time to be learnt or that a basic acoustic knowledge is sufficient to successfully use them. However, in reality, most of these software tools require extended training whenever the user wants to go deeper into their different features – in conflict with the student's tight timing and planning for laboratory and theory sessions. Therefore, to overcome this limitation, by using PARDOS, unexperienced students can undertake complex simulations in minutes, in stark contrast to the other software packages [19], [23]–[25].

The tool hereby presented has been optimized to provide fast, accurate and reliable results of complex scenarios – the design of any obstacle can easily be developed using the proper combination of wedges, rectangles, cylinders, and T/Y-shaped structures – in such a way that the average simulation time can perfectly match the usual duration of constrained laboratory sessions many subjects are limited to.

PARDOS, therefore, represents a contribution to the application of educational software in the field of Acoustics, being aimed at a prediction and analysis of the complex sound pressure field existing at any receiver's (listener's) location, incorporating any two-dimensional (2D) scenario defined and loaded by the students. Furthermore, unlike purely professional acoustic software, the tool presented here includes four guided practice exercises for the students to perform. Additionally, PARDOS allows for saving all the calculations (scenarios, environment, IL, attenuation, acoustic sources, impulse response, etc.), to simulate the expected received sound when injecting an audio file as the source (auralization module), or to display sound pressure level (SPL) maps, to plot the possible paths from the source to the receiver, and many other features. The MATLAB programming environment further allows the capabilities and utilities of PARDOS to be fully exploited, such as through the use of a large database of built-in algorithms and toolboxes, image processing, external libraries, extensive data analysis and visualization tools, friendly graphics user interfaces, easy development and debugging of code, and speed and reliability. Moreover, students are usually quite familiar with this language, meaning the results can easily be processed, analyzed, compared, stored, or exported at the user's discretion. The MATLAB programming environment, therefore, allows for more efficient management and representation of the results obtained.

Finally, the practice exercises that PARDOS incorporates – which could be part of syllabuses focused on Acoustics – have been adapted from real environments (e.g. road traffic noise, or sound propagation in a factory or a theater). In any case, this software tool gives the user the flexibility to create new scenarios by considering the polygonal structures that best fit the geometry of the environment to be analyzed, as well as permitting the specification of the densities and acoustic impedances of the obstacles' faces, floors, and ceilings (for indoor cases).

The paper is outlined as follows: Section II introduces the terminology, fundamentals, and routing algorithms as well as a Graphical User Interface (GUI) insight where the options and capabilities (inputs, calculations and results) of PARDOS are reviewed; Section III describes four guided activities with incremental difficulty to be carried out by students during laboratory sessions; finally, Section IV presents the authors' conclusions.

II. PARDOS SOFTWARE TOOL

A. PROPAGATION MODEL. FORMULATION

The method implemented in PARDOS is based on an innovative two-dimensional (2-D or 2.5 D if we take the ground or ceiling reflection into consideration) formulation founded in UTD to analyze multiple diffraction/reflection of acoustic waves; the authors have demonstrated, made comparisons, and validated such formulation in [22]. This UTD methodology is enhanced by using graph theory, Fresnel ellipsoids, and funicular polygons so that consideration is only given to those paths and obstacles in this complex environment that make a contribution to global IL. This allows for the provision of swift, accurate, and efficiently computed predictions for sound attenuation, something that cannot be achieved employing alternative more time demanding techniques, e.g. Boundary Element Method (BEM). Using this technique, a substantial quantity of obstacles (which includes adjacent ones of the same height) may be managed in high-frequency resolution and in a sufficiently short time. We can model the obstacles as cylinders, rectangles, wedges, or knife edges, and

also as a number of other polygonal deflecting obstacles, e.g. T-or Y-shaped barriers or trapezoids.

In this manner, the total diffracted (and reflected on ground/floor) complex pressure field emanating from a source S at any frequency to the receiver R will represent the entirety of the rays converging on R on every possible path:

$$\phi_{t_{Rx}} = \sum_{i=1}^{n} \phi_{path\,i}\,(S, R)\,, \tag{1}$$

where $\Phi_{path\,i}$ (S, R) is the complex received field from S to R following the path *i*. It is assumed that S is a point source generating spherical wave fronts in an isotropic (uniform) medium, e.g., air, whilst the receiver of this acoustic field R has an isotropic pattern of unity gain. The phase is considered for every signal on every path relying on the UTD theory and combining the diffraction phenomenon with ray representation. A loop then runs each bin of the whole band to derive the total sound pressure field for the full set of paths on a specific frequency. With every frequency, the algorithm further permits checking of sound pressure field levels for every path at the receiver. With sorting of the set of paths, it is predicted that the derived sub-fields will progressively decrease, defining an adjustable pressure condition which can block new fields from being added when the current field does not meet the threshold. We may define the threshold as being the absolute value for the ratio between signal level received on the current path and frequency and the cumulative signal level received at the present frequency (e.g., 1 x 10^{-5}). When the threshold level is set at -1 this ensures that no path is discarded. It is important to note that the compensation time for this suggested algorithm is independent of frequency and may be restrained or limited at any time, as worst-case scenarios can be predicted through multiplication of consumed times at any frequency by the quantity of frequency bins under consideration in the simulation.

Fig. 1 summarizes the flow chart of the software tool's core to obtain the Sound Pressure spectrum:

Therefore, PARDOS allows for different strategies to control and constraint the number and angle of beams in order to prevent computational slow calculations which, on the other hand, do not significantly improve the accuracy of the result. Such strategies are: setting the maximum number of hops from the source to the receiver; adjusting the threshold ratio to prevent the addition of much weaker signals from any path to the accumulated complex sound pressure signal; disabling or enabling ground/reflection effects; modifying a semi-operational setting to restrict the number of ceiling nodes (200 is set by default).

PARDOS tool launches the beams just to the selected reflecting (ground or ceiling) or diffracting (obstacles) nodes, according to the sorted list of paths found by means of the *Breadth First Search* method. So, the number of beams or paths is not established by the users but automatically obtained by the tool.

The process followed by PARDOS to get the final filtered nodes and paths between the source and receiver in each

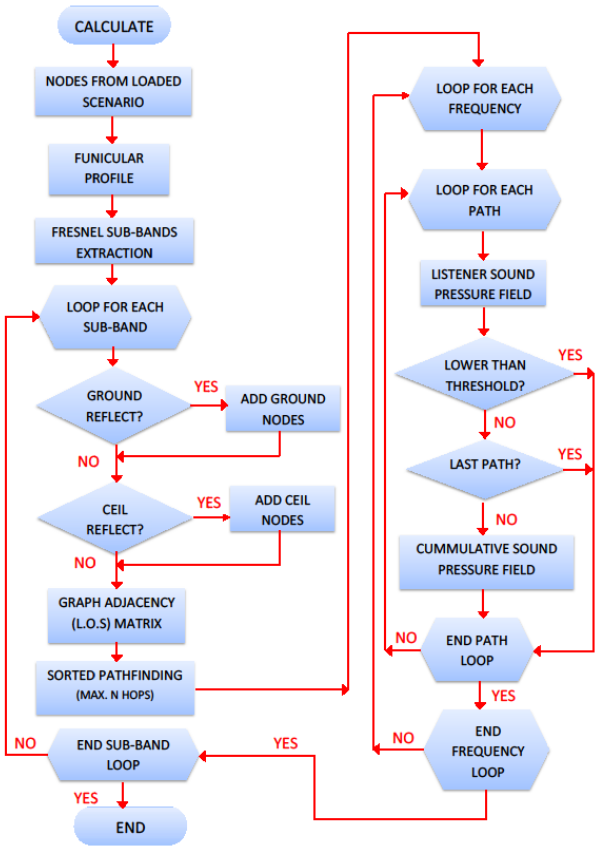

FIGURE 1. 'Calculate' subroutine flow diagram.

frequency band is widely explained in [22]. Once the scenario is loaded (Fig.2a), the following steps take place per each Fresnel frequency band: identification and filtering of obstacle nodes (Fig. 2b); search of ground and ceiling nodes by the IS method, filtering by Line of Sight (LOS) criteria and addition to the set of nodes (Fig. 2c); building of the LOS Matrix from selected nodes, pathfinding, sorting of paths from the shortest to the longest one, calculation of losses, and plot of the selected paths (Fig. 2d).

The complex field at the receiver for all frequencies and all paths may be achieved using the following expression:

$$\phi_{path\,i} = \frac{\phi_0}{s_T} \cdot e^{-jks_T} \cdot \prod_{n=1}^{N-2} \left(\frac{D_n}{R_n}\right) \cdot \sqrt{\frac{s_T}{\prod_{j=1}^{N-1}(s_j)}} \cdot \gamma \cdot e^{-s_T} \tag{2}$$

where:

ϕ_0 represent the SPL from the source;

$s_T = \sum_{j=1}^{N} s_j$, with s_j representing the slant distances for the links of paths chosen, between each node's geometrical centers;

N represents the quantity of nodes for every path;

k represents the wavenumber;

D_n represents the diffraction coefficient and R_n the reflection coefficient; application is dependent on the form of incidence either obstacle or ground;

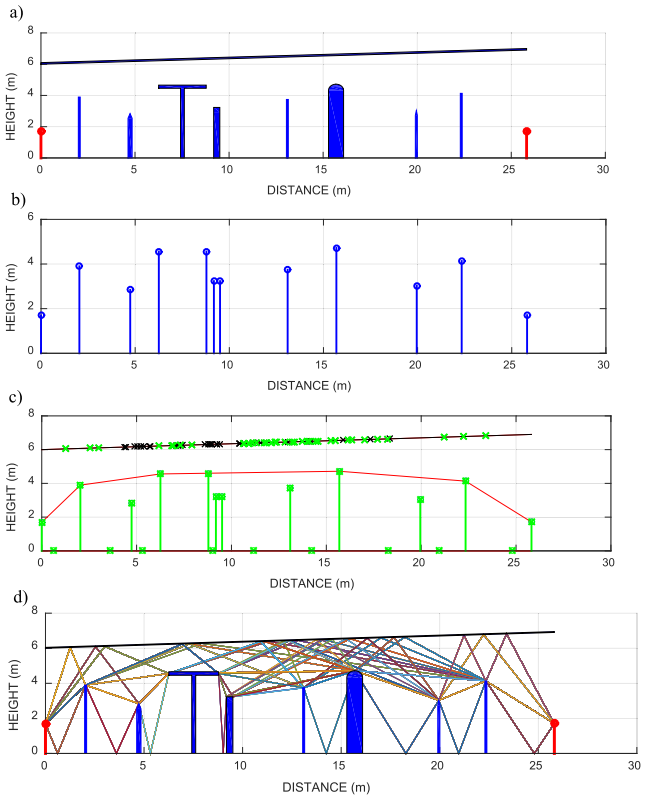

FIGURE 2. a) Scenario loading, b) obstacle nodes selection, c) search of ground and ceiling nodes (in green), d) plot of selected paths.

γ represents the obstacle coefficient factor. The expression derives from [26] and [27] but includes, in this instance, the γ coefficient factor for two reasons: for adjusting the phase, and to be a weight factor ([28], [29]), for every form of obstacle under consideration in this research.

α is the air-absorbent coefficient in Np/m, according to [30]. In turn, this parameter depends on the following input variables, which are related to the source's frequency emission (f) and the physical properties of the air: static pressure (Ps), Celsius temperature (T), percentage relative humidity (H).

1) PRESSURE DIFFRACTION COEFFICIENTS (Dn)

According to UTD [27], the pressure diffraction coefficient for knife-edges and wedges can be defined as:

$$D(v,k,L,s1,s2,\theta_2,\theta_1) = \frac{-e^{-i\frac{\pi}{4}}}{2v\sqrt{2\pi k}} \cdot \begin{bmatrix} \tan^{-1}\left(\frac{\pi+(\theta_2-\theta_1)}{2v}\right)\cdot F\left(kLa^{+}(\theta_2-\theta_1,v)\right) \\ +\tan^{-1}\left(\frac{\pi-(\theta_2-\theta_1)}{2v}\right)\cdot F\left(kLa^{-}(\theta_2-\theta_1,v)\right) \\ +R_n\cdot\tan^{-1}\left(\frac{\pi+(\theta_2+\theta_1)}{2v}\right)\cdot F\left(kLa^{+}(\theta_2+\theta_1,v)\right) \\ +R_0\cdot\tan^{-1}\left(\frac{\pi-(\theta_2+\theta_1)}{2v}\right)\cdot F\left(kLa^{-}(\theta_2+\theta_1,v)\right) \end{bmatrix} \quad (3)$$

with R_0 and R_n representing the reflecting coefficients for adjacent/opposite obstacle faces seen by the incident wave.

In turn, the reflecting coefficients R_0 and R_n depend on the incident (θ_1) and diffracting (θ_2) angles of the path between the transmitter and the listener, respectively, and the normal specific acoustic impedances of the faces seen by them (Figure 3) ([27] offers greater detail regarding the other parameters).

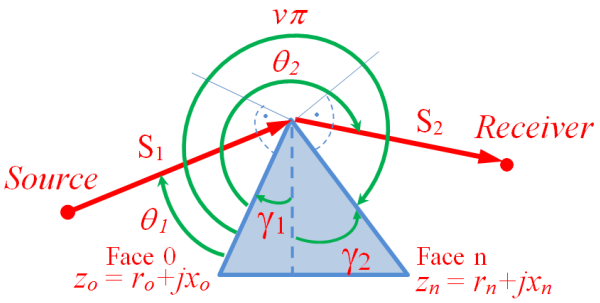

FIGURE 3. Notation used in a single diffracting wedge.

F[x] represents the "transition function", which can be defined as a Fresnel integral [27]:

$$\mathrm{F}[\mathrm{x}] = 2\mathrm{i}\sqrt{\mathrm{x}}\mathrm{e}^{\mathrm{ix}}\int_{\sqrt{\mathrm{x}}}^{\infty}\mathrm{e}^{-\mathrm{iu}^2}\mathrm{du}, \quad (4)$$

$$\mathrm{L} = \frac{\mathrm{s_i s_j}}{\mathrm{s_i}+\mathrm{s_j}}, \quad (5)$$

and

$$\mathrm{a}^{\pm}(\beta) = 2\cos^2\left(\frac{2\mathrm{v}\pi\mathrm{N}^{\pm}-\beta}{2}\right), \quad \beta = \theta_2 \pm \theta_1, \quad (6)$$

where $\mathrm{N}^{\pm}$ are the integers which most closely satisfy the equations

$$2\pi\,\mathrm{vN}^{+}-\beta = \pi, \quad (7)$$

$$2\pi\,\mathrm{vN}^{-}-\beta = -\pi. \quad (8)$$

In the same way, we may employ UTD for explanation of the diffraction coefficient with cylindrical structures using a pair of scattering mechanisms, being either the field's diffraction or reflection components [31]–[33]. Thus with the "shadow region" (source-receiver Line of Sight (LOS) absent) we may consider this diffraction coefficient:

$$T_{s,h}(a) = m_p\sqrt{\frac{2}{k}}e^{-i\frac{\pi}{4}}e^{-ikt(a)}\left\{\frac{-F[x(a)]}{2\varepsilon(a)\sqrt{\pi}}+\left[q^{*}(\varepsilon(a))\right]\right\}, \quad (9)$$

where

$$\mathrm{a} = \pi+\alpha+\beta, \alpha, \beta \geq 0, \quad (10)$$

$$x(\mathrm{a}) = \frac{\mathrm{kL}(\mathrm{a}-\pi)^2}{2}, \quad (11)$$

$$\varepsilon(\mathrm{a}) = \mathrm{m_p}(\mathrm{a}-\pi), \quad (12)$$

$$\mathrm{m_p} = \left(\frac{\mathrm{k}\cdot\mathrm{r_{obs}}}{2}\right)^{\frac{1}{3}}, \quad (13)$$

$$\mathrm{t}(\mathrm{a}) = (\mathrm{a}-\pi)\,\mathrm{r_{obs}}, \quad (14)$$

where α and β are the angles of the arc run by the 'creeping' wave over the rounded surface, k is the wavenumber, r_{obs} is the radii of the cylinder, and s_i and s_j are the slant ranges from the source and receiver, respectively. A comprehensive description of each variable is also explained in [31]–[33] as well as in [22]. The first addend of Equation (9) describes the said Fresnel diffraction process or ''transition function''.

For the second extension of Equation (9), the term $q*(\varepsilon(a))$ represents the ''Fock scattering function'', which deals with creeping waves generated along a smooth body's surface, e.g. spheres or cylinders [32]. In the same way in the ''lit region'' (source/receiver Line of Sight), we may alternatively apply this diffraction coefficient:

$$R_{s,h}(a) = \sqrt{\frac{r}{m'}} e^{-i\frac{\varepsilon^3(a)}{12}} e^{-i\frac{\pi}{4}} \left\{ \frac{-F[x(a)]}{2\varepsilon(a)\sqrt{\pi}} + \left[q^*(\varepsilon(a))\right] \right\}, \tag{15}$$

where

$$\varepsilon(a) = -2m_p \left(\cos\left(\frac{a}{2}\right)\right), \tag{16}$$

$$X(a) = 2kL \left(\cos\left(\frac{a}{2}\right)\right)^2, \tag{17}$$

with L as in Equation (5), m_p as Eq. (13) and

$$a = \theta_2 - \theta_1. \tag{18}$$

Parameters are similarly detailed in [31]–[33] and in [22].

2) REFLECTION COEFFICIENTS (Rn, Ro)

The method chosen for analyzing the Rayleigh reflection coefficient of waves obliquely incident on the surface of a solid (either on ground, ceiling, or on any obstacle surface) with a known normal-specific acoustic impedance can be reviewed in Chapter 6 of [34]. Providing that the surface is acoustically smooth, without the irregularities of the order of a wavelength in size, sound wave-fronts will not be scattered in other directions and will be reflected as largely intact (Chapter 12 of [35]).

If the speed of sound in air (c_{air}) was higher than that of the solid media (c_{solid}), or if c_{air} was lower than that of solid media but the angle of incidence θ_i is less than the critical angle θ_c,

$$\theta_c = \text{asin}\left(\frac{c_{air}}{c_{solid}}\right), \tag{19}$$

then the Rayleigh reflection coefficient would be:

$$R = \frac{\frac{r_1}{z_o} - \frac{\cos(\theta_t)}{\cos(\theta_i)} + \frac{jx_1}{z_o}}{\frac{r_1}{z_o} + \frac{\cos(\theta_t)}{\cos(\theta_i)} + \frac{jx_1}{z_o}}, \tag{20}$$

with r_1 and x_1 being the resistance and reactance, respectively, of the complex normal-specific acoustic impedance of the solid material defined as:

$$z_1 = r_1 + jx_1, \tag{21}$$

with z_o being the characteristic impedance of the air, and

$$\cos(\theta_t) = \sqrt{1 - \left(\frac{c_{solid}}{c_{air}}\right)^2 \cdot \sin^2(\theta_i)}, \tag{22}$$

being θ_t the angle of transmission in the solid.

Otherwise, if $c_{solid} > c_{air}$ and under the restriction $\theta_i > \theta_c$, then the reflection coefficient would be:

$$R = e^{i\emptyset}, \tag{23}$$

$$\emptyset = 2 \cdot \text{atan}\left[\left(\frac{\rho_{air}}{\rho_{solid}}\right) \cdot \sqrt{\left(\frac{\cos(\theta_c)}{\cos(\theta_i)}\right)^2 - 1}\right], \tag{24}$$

with ρ_{air} and ρ_{solid} the densities of air and solid, respectively.

Finally, the total sound pressure at the receiver for each frequency will be the summation of all the sound pressure signals for all the selected paths arriving at the receiver, as shown in (1).

B. PARDOS FLOW CHART

The flowchart in Fig. 4 indicates the step-by-step process to be followed in order to obtain the available results with PARDOS.

C. GRAPHICAL USER INTERFACE

Fig. 5 offers a general view of the PARDOS graphical user interface (GUI):

Step-by-step menus for sound propagation calculations with PARDOS are described in the following sections:

1) INPUTS

Air Physical Properties (Fig. 6): Air characteristic impedance (rayls); Air Temperature (° Celsius); Air Pressure (Pa); Air Relative Humidity (%); PARDOS automatically updates and displays the speed of sound (m/s) and air density (kg/m^3) based on the last three variables indicated above (temperature, pressure, and humidity), following [10]. PARDOS will also consider the specific speed of sound associated with each frequency to calculate the attenuation and absorption losses spectrum. The speed of sound input label in Fig. 5 will only display the value for the average range frequency selected by the student.

Global Simulation Parameters (Fig. 7): The maximum number of hops allowed between the scenario's source and listener nodes, in order to constrain the contributions of signals that have followed extremely long paths and, therefore, with negligible signal levels; (Signal) Threshold level, which is a criterion for interrupting the simulation for the weakest signal paths and stands for the current signal pressure to cumulative signal pressure for each frequency bin (e.g. 10^{-5}); Number of frequency bins (resolution); Minimum sub-band percentage. This input allows for controlling the minimum analysis sub-band using the Fresnel criteria [5]. In order to optimize computation time, PARDOS recalculates relevant nodes, the Line of Sight (LoS) matrix, and paths for each sub-band. The minimum sub-band provides a balance to ensure

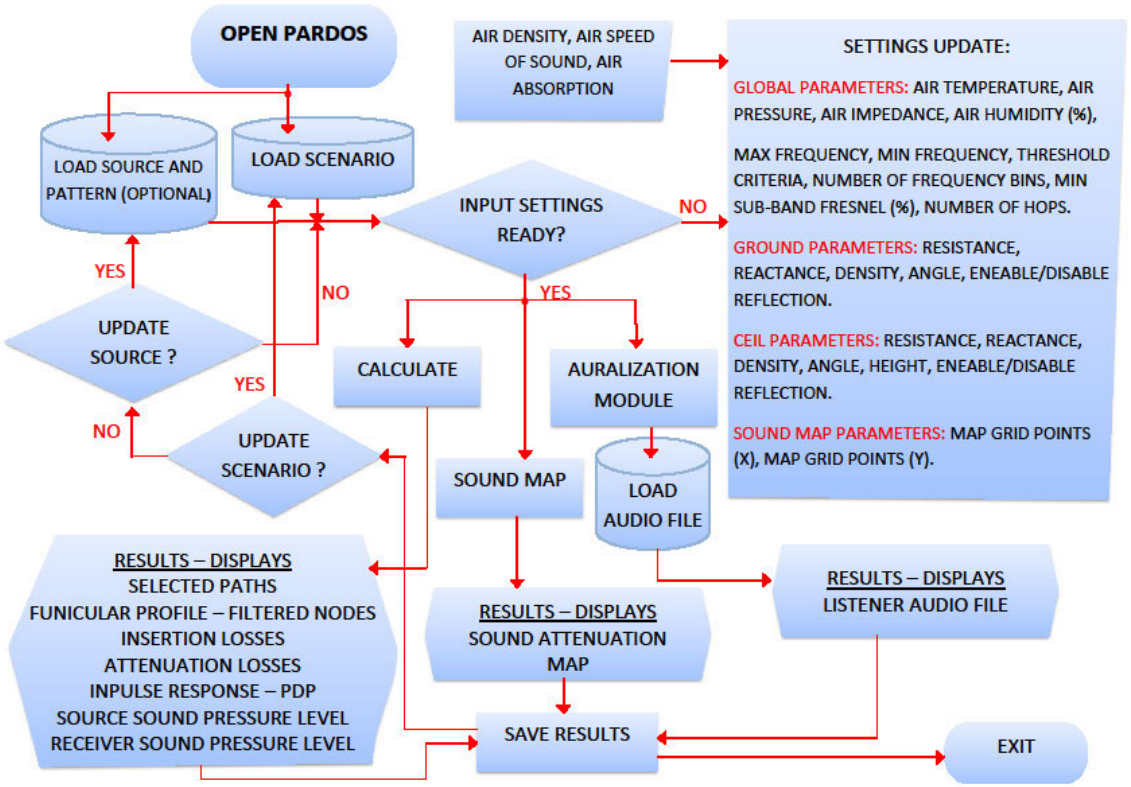

FIGURE 4. PARDOS flow diagram.

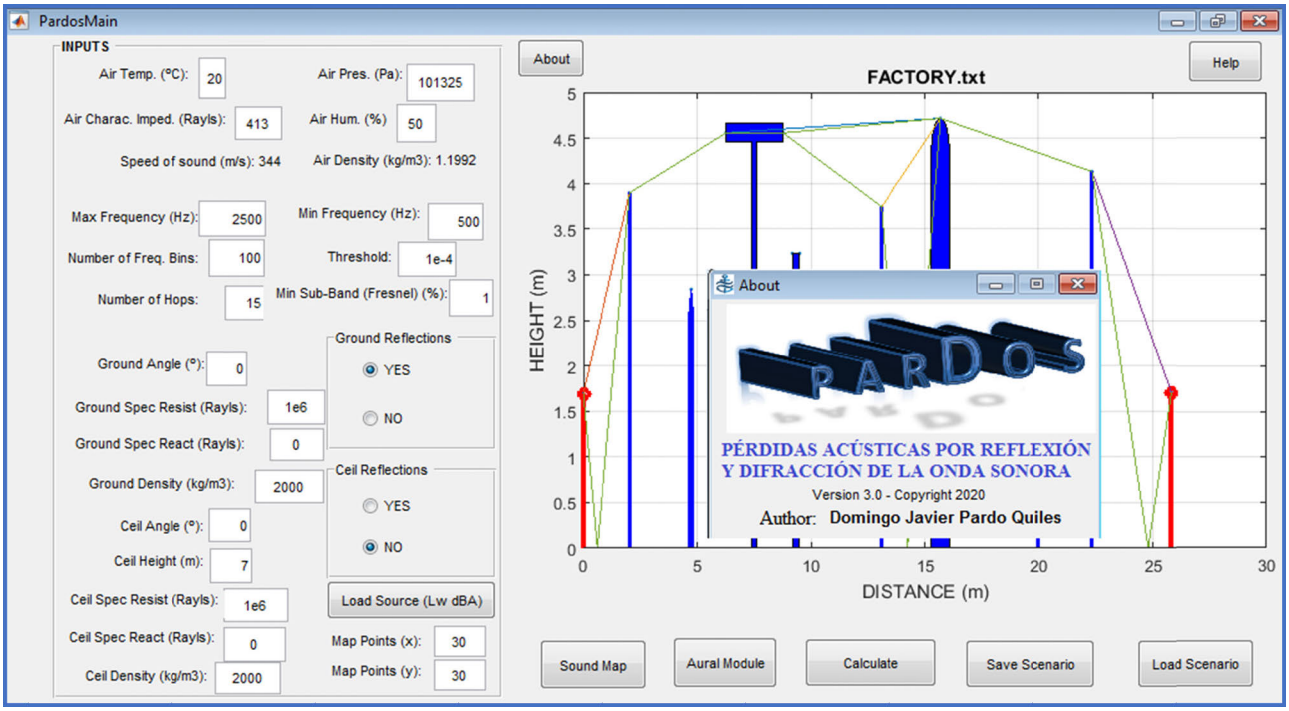

FIGURE 5. PARDOS main GUI with 'About' pop-up window.

that too much computation time is not spent on just a few frequency bins.

Ground Parameters (Fig. 8): Graphical User Interface (GUI) for entering the ground angle (°); Ground-specific

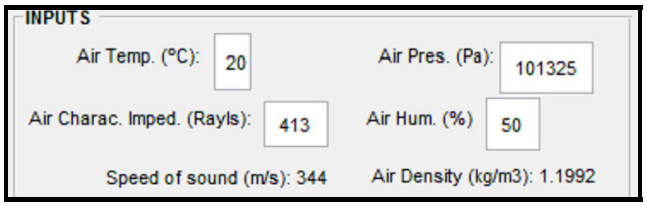

FIGURE 6. Air physical properties.

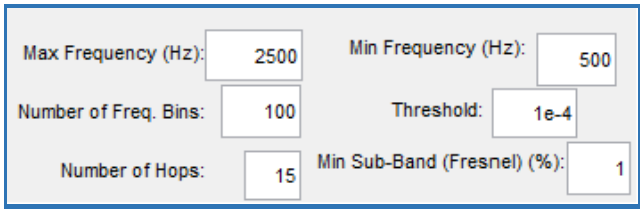

FIGURE 7. Global Simulation Parameters.

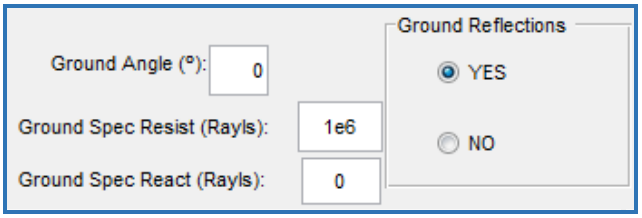

FIGURE 8. Ground Parameters.

resistance (Rayls); Ground-specific reactance (Rayls); Ground density (kg/m^3); Radio-buttons to enable or disable ground reflection evaluation.

Ceiling Parameters (Fig. 9): GUI for entering the ceiling angle (°); Ceiling-specific resistance (Rayls); Ceiling-specific reactance (Rayls); Ceiling density (kg/m^3); Radio-buttons to enable or disable ceiling reflection evaluation.

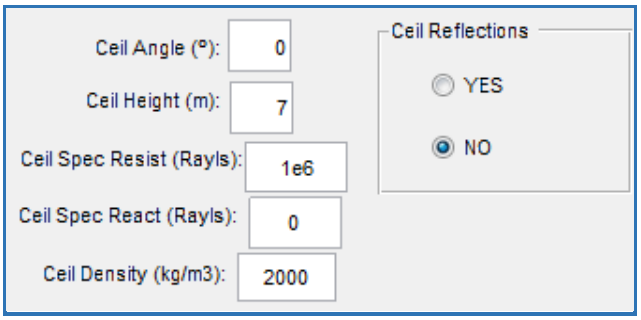

FIGURE 9. Ceiling parameters.

Load Source (Fig. 10): Sound Power Level and SPL, with A-weighting (see Fig. 10 for an example).

Load Source Pattern (Fig. 11): Linked to the definition of the source spectrum is the selection of the acoustic source pattern. Students can define it using only a text file with two rows, whereby the first row stands for the angles (in degrees)

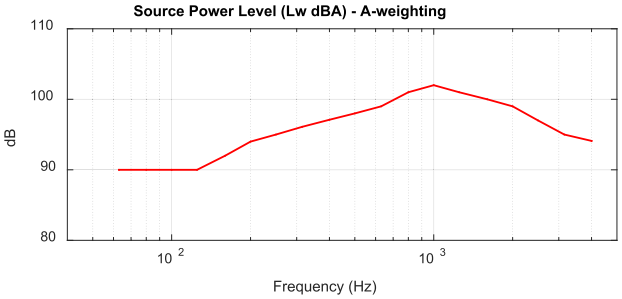

FIGURE 10. Source Power Level (Lw dBA) with A-weighting.

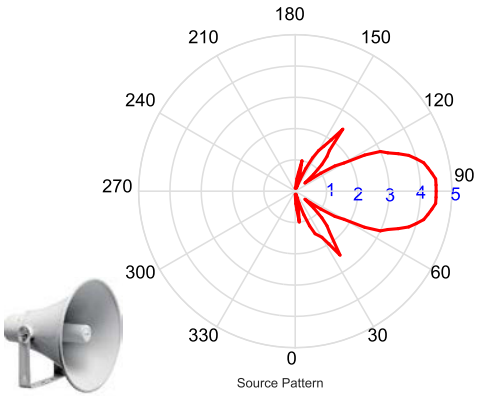

FIGURE 11. Source Pattern. Example of a directional source.

and the second row is the gain in linear magnitude. An omni-directional pattern is set by default.

Load Scenario: The scenario under analysis can be created with any text editor application, such as Notepad@ or Wordpad@. The file should be a matrix of 12 rows by N columns (with N being the number of structures, including obstacles, source, and receiver), without any label or header and separated by spaces. The order of inputs for the scenario should be as shown in Table 1.

TABLE 1. Example of a scenario created with a text editor.

1	Height (H)	0.5 2.5 3.5 3.0 4.0 3.0 2.0 3.0 2.0 0.6
2	Distance (D)	0 3.5 4.5 6.0 7.5 10 12.3 13.0 15.2 18.0 21.0 22 25.0
3	Node Type (T)	0 6 7 4 2 2 89 4 2 2 2 0
4	Left Angles (γ_1)	0 0 90 0 0 40 0 90 0 0 30 0 0
5	Right Angles (γ_2)	0 90 0 0 0 60 90 0 0 0 20 0 0
6	Radius (r)	0 0 0 0.4 0 0 0 0 0.2 0 0 0 0
7	Left Spec. Ac. Resist (R_1)	0 1e6 1e6 1e6 1e6 1e6 1e6 1e6 1e6 1e6 1e6 1e6 0
8	Left Spec. Ac. React (X_1)	0 0 0 10 0 0 0 05 0 0 0 0
9	Right Spec. Ac. Resist (R_2)	0 1e6 1e6 1e6 1e6 1e6 1e6 1e6 1e6 1e6 1e6 1e6 0
10	Right Spec. Ac. React (X_2)	0 0 0 2 0 0 0 0 7 0 0 0 0
11	Left Densities (d_1)	0 200 100 200 500 800 300 100 1000 150 100 200 0
12	Right Densities (d_2)	0 200 100 200 500 800 300 100 1000 150 100 200 0

Note: The explanatory text in blue is not part of the content of the file and is only intended to clarify each row of the data matrix.

The appropriate codes for the field Node Types (line 3 in Table 1), as well as the number of nodes for obstacles, source, and receiver are detailed in Table 2.

A double-inclined barrier is treated as a wide barrier where the 'face' on the right is fully absorbing (reflection coefficient is set to 0). For this purpose, the 'virtual' face on the right of

TABLE 2. Codes and number of nodes for obstacles, source, and receiver.

	Type (Reserved Ranges)	Number of Nodes
Source and Receiver	0	1
Edges	2	1
Wedges		
Cylinders	4	1
Rectangle, Double Inclined	6 -7, 8-9, …, 98-99	2
T-shaped	100-101, 102-103, …,198-199	2
Y-shaped	200-2-201, 202-2-203, … ,298-2-299	3

this obstacle is created by considering the same air density and impedance.

Left angles and right angles stand for the angle of the faces of any node of each obstacle [5]. For transmitter, receiver, edges, and cylinders, both angles are fixed to 0°. Wedges are built with just 1 node with both left and right angles (aperture) being selectable. For other obstacles with several nodes, the angles are in accordance with Table 3.

TABLE 3. Right and left angles for each type of node.

	First node Left $\gamma 1$– Right $\gamma 2$ Angles (°)	Second node Left $\gamma 1$– Right $\gamma 2$ Angles (°)	Third Node Left $\gamma 1$– Right $\gamma 2$ Angles (°)
Rectangle	0° – 90°	90° – 0°	N/A
T-shaped	0° – 90°	90° – 0°	N/A
Y-shaped	0° - $\gamma 2$	0° – 0°	$\gamma 1$ – 0°
Double Inclined	$\gamma 1$ – 90°	90° – 0°	N/A

Other types of obstacles can be built by combining the polygonal shapes referred to previously.

Save Scenario: By pressing the Save button, the student is given the option to save all the results obtained, including the simulation parameters applied and the chosen scenario. Furthermore, the figures presented by PARDOS can be saved in any of the image formats desired by the student (bmp, eps, jpeg, pcx, tif, etc.) or as a pdf.

Help: Pressing the Help button opens a complete tutorial on the use of this tool. In addition, students can access a set of four guided practice exercises.

2) CALCULATIONS

Calculate: After pressing the Calculate button, the software tool will run each frequency bin to obtain the sound pressure field at the receiver. The computation time is constrained and controlled by the maximum number of hops, the resolution (frequency bins), the minimum sub-bands (%), and the threshold defined as apart from the scenario's complexity.

Auralization Module: This module allows for loading any.wav audio file as the source and simulates the expected sound at the listener's position once the impulse response of the 'channel' (scenario) has been calculated. The users can then save the resulting audio file at the receiver, then subsequently play it to check for sound quality – this allows for analyzing, for example, the significant presence, or not, of reverberation. This could provide a valuable tool, therefore, for assessing the subjective quality of sound at the listener's position.

Sound Map: With this option, the users can create a map of both the IL and attenuation levels at any frequency entered in the Fmax input using the resolution grid defined by xmap and ymap input parameters. The users must select the insonified area of the map by clicking on the left upper corner and right down corner of the desired region conforming to the map.

3) OUTPUTS. RESULTS

Pathfinding Display (Fig. 12): Funicular Profile and node filtering process (if the clearance of the Fresnel ellipsoid between two adjacent funicular nodes remains unobstructed with respect to the height of one intermediate obstacle, then such an obstacle will be discarded for diffraction loss calculation purposes [5] – Fig. 13):

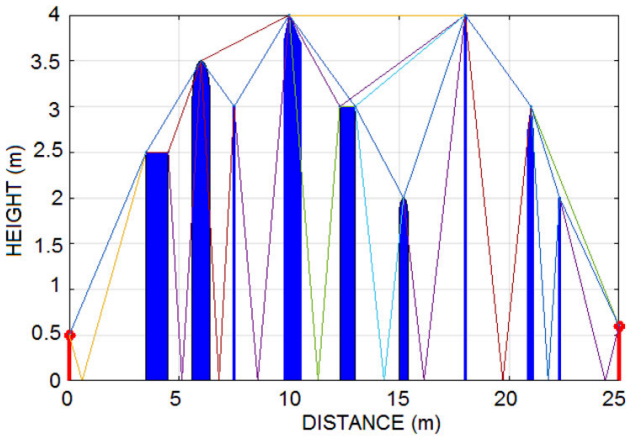

FIGURE 12. Example of Pathfinding.

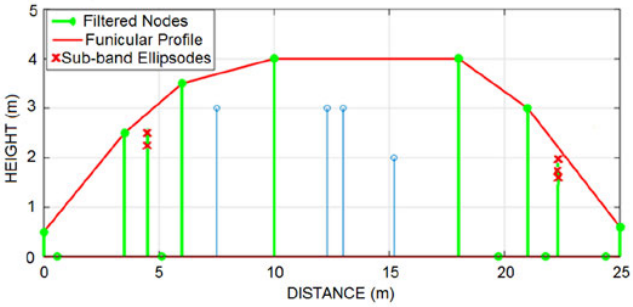

FIGURE 13. Funicular profile, filtered nodes (in green), and sub-band ellipsoids progress (red crosses).

IL (dB) at the listener position, as a function of frequency (Fig. 14):

Attenuation(dB) sound pressure field spectrum at the listener's position (Fig. 15):

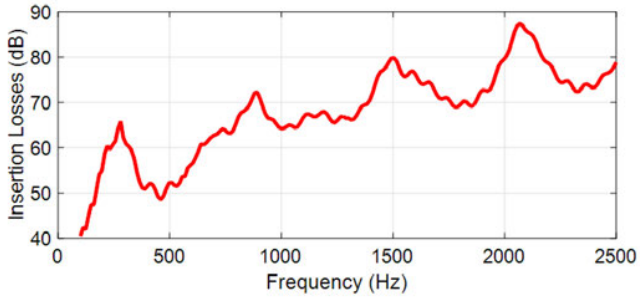

FIGURE 14. Example of IL spectrum.

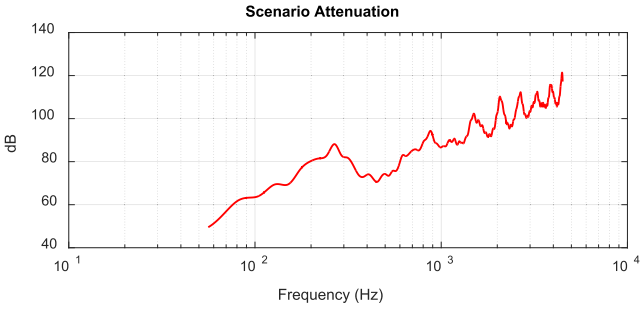

FIGURE 15. Example of sound attenuation spectrum figure with a logarithmic axis for frequencies.

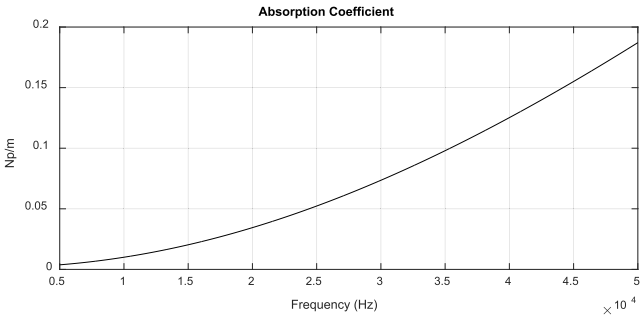

FIGURE 16. Example of Sound Absorption coefficient.

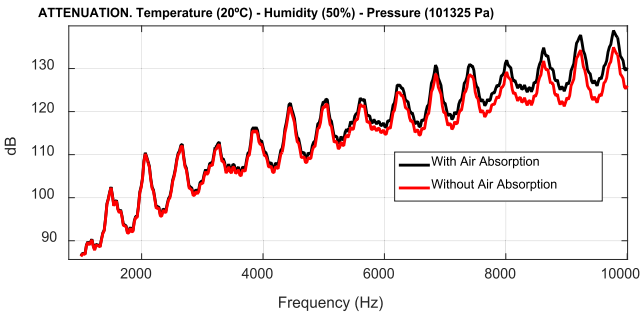

FIGURE 17. Example of sound attenuation spectrum at the listener's position with and without air absorption.

Students can also check the influence of the air absorption coefficient (Fig. 16) on the global attenuation in such a manner that a comparison with and without this coefficient can be jointly displayed and compared (Fig. 17).

Source SPL (dBA) (Fig. 18):

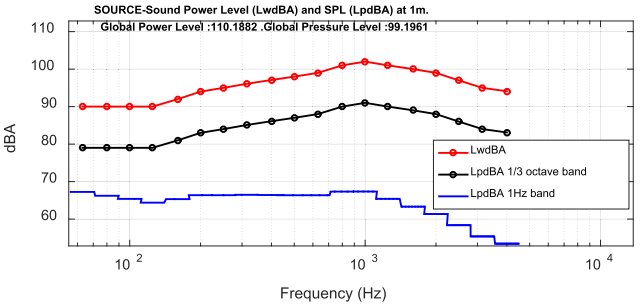

FIGURE 18. Source Sound Pressure and Power Levels.

By means of this figure, the students can verify the sound power and pressure spectrum of the selected source.

Receiver SPL(dBA) (Fig. 19):

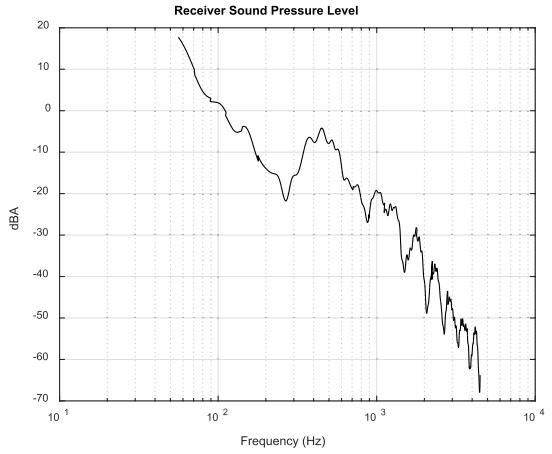

FIGURE 19. Receiver SPL spectrum.

This plot also provides the global Sound Power Level as well as the SPL spectrum.

Power Delay Profile. Impulse Response (Fig. 20):

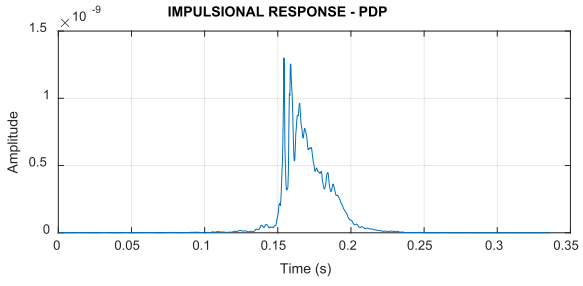

FIGURE 20. Impulse response as a function of time.

This plot allows for knowing the effect of the multipath and sound dispersion of the wave arriving at the receiver.

Sound Attenuation Map (Fig. 21):

This plot can be obtained from the Sound Map module.

Sound IL Map (Fig. 22):

As in Fig. 21, this plot is provided by the sound map tool.

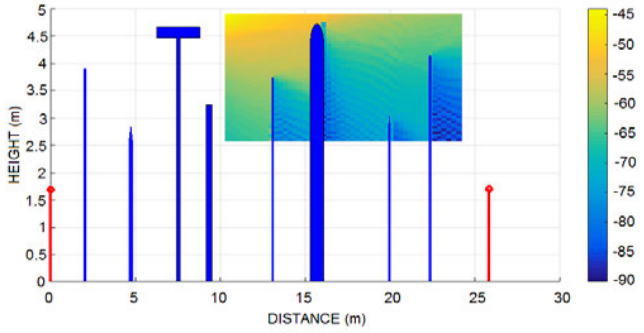

FIGURE 21. Sound attenuation map at 1,500 Hz.

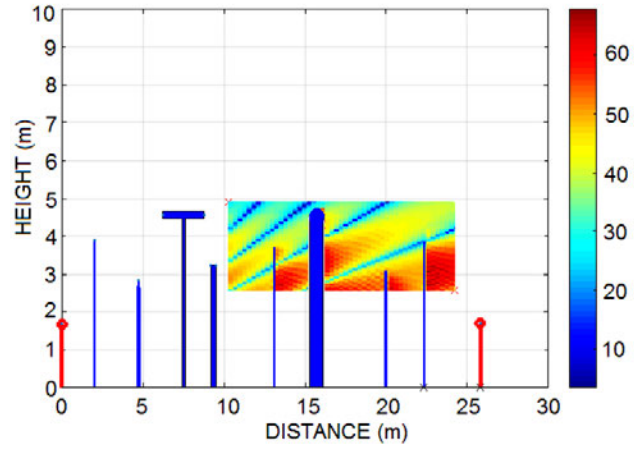

FIGURE 22. Sound Insertion Loss map at 1,500 Hz.

III. GUIDED PRACTICES USING PARDOS

As mentioned before, as part of its Help/Tutorial section, PARDOS includes a set of four practice exercises with corresponding instructions to guide students in properly fulfilling their objectives during eventual Laboratory Sessions. In this sense, such practices are set out to last less than 1 hour and 30 mins – explored in the following section.

The competences and skills that are expected to be acquired throughout the four following practice activities are:

1. To understand the fundamentals of acoustic propagation as well as the multiple factors involved in the final response.
2. To create and explore real simulated outdoor and indoor scenarios.
3. To optimize acoustic environments (e.g. by selecting material impedance and densities).
4. To adhere to acoustic requirements and/or architecture restrictions (e.g. ceiling height, floor angle, listener maximum distance, etc.).
5. To auralize scenarios and listen to the simulated response, reverberation effects, and feeling of immersion.
6. To increase motivation to face the resolution of new challenges and problems in the field of acoustics.

A. PRACTICE 1. INTRODUCTION TO PARDOS

The goal of this practice is to train the students in the handling of the different PARDOS tools, options, and plots available. This way, the students will reinforce Competence 1 by reviewing key acoustic terms (attenuation and IL, impulse response, diffraction loss for different obstacles), as well as Competence 2, when creating new scenarios by the addition of cylinders, wide barriers, wedges, etc. to the simple free-space loss outdoor case.

This way, at the end of the practice, the students will have gained familiarity with this software tool. They will be able to create scenarios and sources, tune the different options and parameters, and shed light on the results.

1. Open the PARDOS tool from the MATLAB environment.
2. Load the scenario "Free of obstacles." This profile is the simplest and most trivial case, including just the source (with a height of 3 m) and the receiver (with a height of 2 m and located 3 m from the source). The scenario can be opened with the text editor so the file format can be reviewed.
3. Disable ceiling and ground reflections.
4. Update parameters in accordance with Table 4.

TABLE 4. Parameters.

Parameter	Value
Speed of sound (m/s)	341
Air Density (kg/m^3)	1.2250
Air Charact. Impedance (Rayls)	413
Min Freq. Band	10 Hz
Max Freq. Band	10000 Hz
Threshold	1e-6
Number of Hops	4
Number of Freq. bins	1500
Min. Sub-band (Fresnel) (%)	5

5. Press the Calculate button.
6. Analyze and comment on the results.
   a. Why are the IL equal to 0 dB, but not the attenuation losses? Check that the expected theoretical attenuation losses A(dB) are the same as the simulated ones (Fig. 23).
   Consider the following equation:

$$A\,(dB) = 20 \cdot \log\left(\left|\frac{Et}{\frac{Et \cdot e^{-ikr}}{R}}\right|\right) = 20 \cdot \log\left(|R|\right) \tag{25}$$

   with Et being the Sound Pressure field transmitted by the source, R the slant range between source and listener, and k the wavenumber.
   b. Why is there no dispersion in the Impulse Response? Check that the time delay τ of the

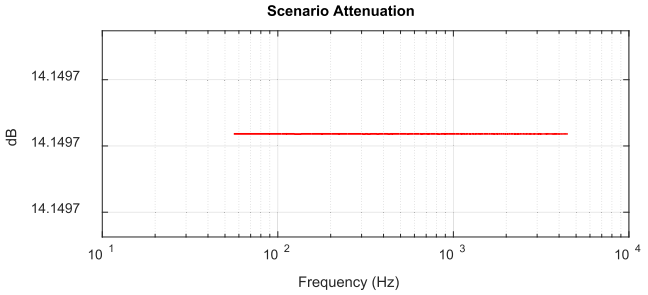

FIGURE 23. Expected attenuation.

signal arrival is coherent with the simulated value (Fig. 24).

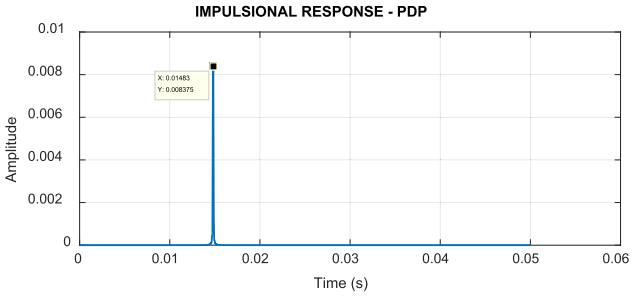

FIGURE 24. Impulse Response.

Note for the professor:

$$\tau = \frac{R}{c} = 14,95\text{ms} \tag{26}$$

with R and c being the straight slant range between source and listener, and the speed of sound, respectively.

7. Enable ground reflection and repeat the calculations. Comment on the results. How does the impulse response look now and why? How do the new IL look?
8. Load the following scenarios with one single obstacle available from the scenarios folder (1 edge, 1 wedge, 1 rectangle, 1 Y-shaped structure, 1 T-shaped structure, 1 Cylinder, and 1 Double-inclined barrier).
9. Calculate and check the IL, attenuation, impulse response, and SPL at the receiver for each scenario. What differences appear among the different obstacles?
10. Modify the existing scenarios using any text editor in order to create a new one with a combination of the basic shapes mentioned:
    a. Scenario with 3 cylinders.
    b. Scenario with 2 wide barriers, 1 double-inclined barrier, and 1 T-shaped structure.
    c. Scenario with 2 wedges, 1 cylinder, 2 T-shaped structures, 2 wide barriers, and 2 Y-shaped structures.

B. PRACTICE 2. ANALYSIS OF AN OUTDOOR REAL SCENARIO. ROAD TRAFFIC NOISE

A common outdoor real scenario will be defined and analyzed in this practice. The students will be able to study, design, and optimize acoustic plain noise barriers fitted with double diffracting caps (attached to the top of the barrier) built in the proximity of roads to mitigate the influence of traffic noise coming from a vehicle.

From an educational point of view, the students will deepen the following Competences: 1, by reviewing acoustic parameters such as Sound Power Level or the impulse response of outdoor scenarios and assessing the influence on the IL of different types and number of diffracting obstacles; Competence 2, when creating new scenarios by adding diffracting elements on top of conventional plain barriers, increasing its height or varying the angle of the ground; Competence 3, by modifying the densities and impedances of the said diffracting devices to enhance their attenuation; and Competence 4, when dealing with acoustic requirements stated by the World Health Organization WHO.

The goal is then to enhance the abatement of the sound coming from vehicles with sirens, such as ambulances, to a residential area located close to the road.

1. Open PARDOS from the MATLAB environment.
2. Create different scenarios with double caps barriers (diffracting elements) attached to the top of a barrier of 3 m height. The noise source (Tx) will be located at a height (h_{tx}) of 2.5 m. The barrier is positioned at a distance (d_1) of 3 m from the sound source and a height (h_{bar}) of 3 m, with a width (w) of 0.4 m. The sound receiver (listener, Rx) will be positioned at a distance (d_2) of 7 m from the barrier with a height of $h_{rx} = 1.7$ m (Fig. 25).

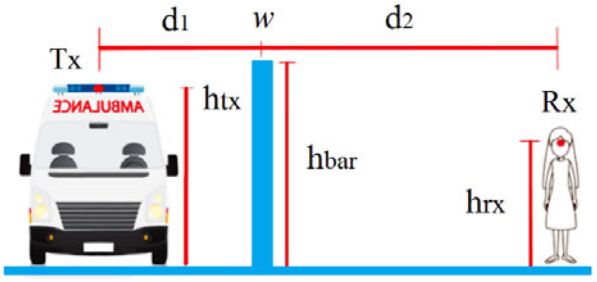

FIGURE 25. Road barrier with ambulance siren (source) and listener.

The barriers (caps) will be built with T-shapes, Y-shapes, cylinders, rectangles, and double-inclined structures, as shown in Fig. 26.

3. Load the Source 'Ambulance.' The spectrum belongs to a vehicle fitted with a siren.
4. Insert the settings as shown in Table 5, or update accordingly.
5. Press 'Calculate' for the scenarios created.
6. Check all the results obtained (IL, Attenuation, Global SPL, filtered nodes and paths, etc.). Comment on the results.

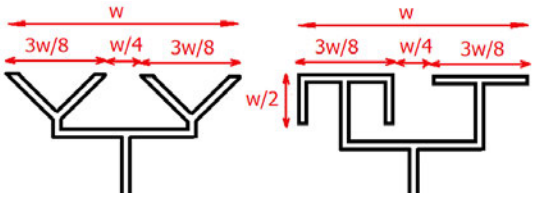

FIGURE 26. Double caps with polygonal shapes.

TABLE 5. Settings.

Parameter	Value
Speed of sound (m/s)	345
Air Density (kg/m^3)	1.2250
Air Charact. Impedance (Rayls)	413
Min Freq. Band	10 Hz
Max Freq. Band	12,000 Hz
Threshold	1e-5
Number of Hops	8
Number of Freq. bins	1,500
Min. Sub-band (Fresnel) (%)	5
Enable Ground Reflection	YES
Ground Resistance (Rayls)	1e6
Ground Reactance (Rayls)	0
Ground Density (kg/m^3)	2000
Ground Angle (º)	5º
Enable Ceiling Reflection	NO

7. Choose the best combination among those possible to enhance the barrier's IL. (Note: it is expected that the double Y cap will be the optimum one – Figs. 27 and 28).

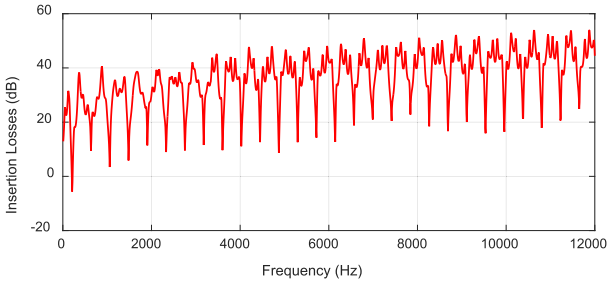

FIGURE 27. IL with a double Y cap on top of the barrier.

8. Confirm theoretically that the arrival of the signals to the listener is coherent with the Impulse Response (assuming double Y cap) (Fig. 29).
   For the optimum configuration, and considering that the Global SPL is higher than 55 dB(A) – considered by the WHO to be a "serious annoyance, daytime and evening, for outdoor living areas," – it is required for the student to alternately implement the following additional measures to comply with the WHO recommendations:
   a. Increase the height of the barrier (no higher than 4 m).
   b. Consider a maximum slope of 5° on the ground.
   c. Use absorptive materials on the caps (coating material available with R=100 rayls and X=200 rayls).
9. Verify that each measure leads to the following Global SPL, which are insufficient for meeting the WHO threshold: a. SPL=58.23 dBA; b. SPL=59.82 dBA; c. SPL=61.44 dBA. On the contrary, several measures jointly applied allow the requirements to be fulfilled (e.g. b and c. SPL=53.61 dBA). Explain the strategies taken and comment on the results obtained.

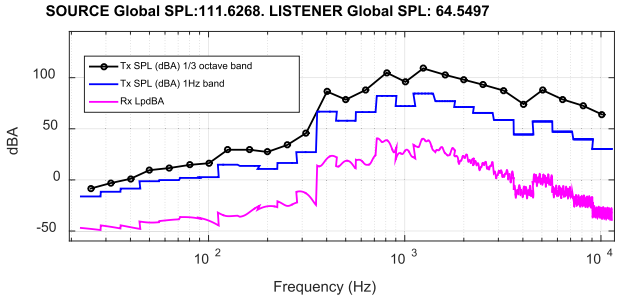

FIGURE 28. Source and listener SPLs (double Y cap).

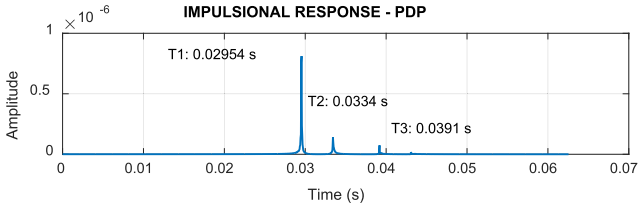

FIGURE 29. Impulse response.

C. PRACTICE 3. ANALYSIS OF AN INDOOR REAL SCENARIO FACTORY

In this practice, the students will be able to analyze the acoustic impact that a receiver will suffer when it is located in the interior of a factory with a noise source – previously loaded as Engine Source. Students will be aware of the influence of the presence of reflecting ceilings versus absorbing ones in the final Global SPL received by the listener.

The competences which are intended to be achieved by the students through the development of this third session will be the same as those of Practice 2: Competences 1, 2, 3 and 4, although applied, in this case, to an indoor environment. In this sense, the students will focus on the marked influence of the ceiling reflections in the global sound pressure regardless the number of diffracting obstacles between the source and listener.

This way, the scenario will consist of a number of reflecting (acoustically rigid) walls with diffracting caps, which will mitigate the sound arriving at the listener.

1. Open PARDOS from the MATLAB environment.
2. Load the Scenario 'Factory.'
3. Load the Source 'Engine 1.'
4. Insert the setting parameters to be as shown in Table 6, or update accordingly.

TABLE 6. Settings.

Parameter	Value
Speed of sound (m/s)	341
Air Density (kg/m^3)	1.2250
Air Charact. Impedance (Rayls)	413
Min Freq. Band	10 Hz
Max Freq. Band	7000 Hz
Threshold	-1
Number of Hops	10
Number of Freq. bins	1500
Min. Sub-band (Fresnel) (%)	5
Enable Ground Reflection	YES
Ground Resistance (Rayls)	1e6
Ground Reactance (Rayls)	0
Ground Density (kg/m^3)	2000
Ground Angle (º)	0
Enable Ceiling Reflection	YES
Ceiling Resistance (Rayls)	1e6
Ceiling Reactance (Rayls)	0
Ceiling Angle (º)	5
Ceiling Height (m)	6
Ceiling Density (kg/m^3)	2000

5. Press 'Calculate.'
6. Check all the results obtained (IL, Attenuation, Global SPL, filtered nodes, and paths – Fig. 30, etc.). Comment on the results.
7. Save the workspace and plots simulated.
8. Now disable the ceiling reflection but keep the ground reflection option, and press 'Calculate' again.
9. In view of the results, analyze whether the ceiling reflection is relevant in terms of IL in spite of having a greater number of walls (acoustic barriers). How could we improve the results?
10. Modify the ceiling density and resistance to increase the absorption. For this purpose, consider a ceiling resistance of 500 rayls and a ceiling density of 200 kg/m^3. Save the results. Create a figure to compare the received SPL in the three considered situations (1: reflecting ceiling, 2: without ceiling reflection, 3: with absorbing ceiling – Fig. 31).

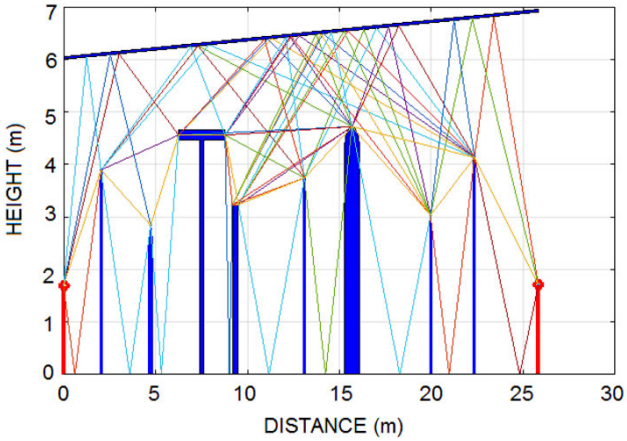

FIGURE 30. Scenario Factory with the pathfinding result.

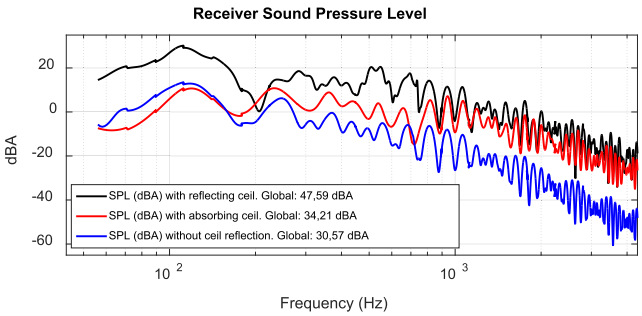

FIGURE 31. SPL with fully reflecting ceiling, absorbing ceiling, and with an absence of ceiling.

11. Comment on the results. Analyze the Impulse responses (PDP), IL, and SPLs.
12. Open the scenario 'Factory' with a text editor and remove the obstacles 2, 4, 5, and 7. Rename the file as 'Factory 2.'
13. Load the scenario 'Factory 2.' Press 'Calculate,' keeping the previous settings of step 10.
14. Comment on the results obtained with this scenario.

D. PRACTICE 4. ANALYSIS OF AN INDOOR REAL SCENARIO. THEATER DESIGN

In this practice, the students will be imitating being commissioned by an architecture studio to optimally design a theater from an acoustics perspective.

This way, the students will enhance Competence 1 when tuning the available PARDOS parameters to reach the desired response; Competences 2 and 3, by exploring and modifying the considered scenario (e.g. changing angles, heights and materials of both ceiling and floor, or the material of the seats of the theater); Competence 4, because the students will pursue the consecution of the requirements imposed by the client; Competence 5, by testing the auralization module to check the reverberation effect; and Competence 6, feeling motivated when coping with problems and alternative ways towards the fulfilment of the goals or when trying to mitigate the well-known 'seat dip effect'.

In this context, it should be taken into account that the brief specifications of the client's technical conditions comprise of the following points:

- Ensure that the acoustic IL have a frequency response as flat as possible, from 100 Hz to 5 kHz.
- Guarantee the presence of LoS from the stage to all attendees.
- Minimize the negative effect of reverberation.
- Constrain the maximum acoustic attenuation at the different rows of the theater stalls.

The supplier is supposed to have provided a 2D drawing of the theater, which is already exported to the PARDOS format in the file '*Theater – 15 rows*' and available in the '*Profiles*' folder.

The students will have to provide a report with at least three alternative designs detailing the results and the assessment obtained to comply with the specifications laid down in the requirements sheet, including recommendations, advantages, and drawbacks, if any, for each option (e.g. Fig. 32).

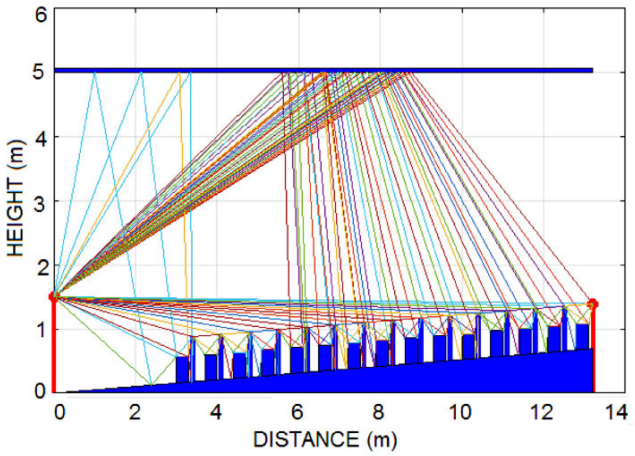

FIGURE 32. Pathfinding analysis in 15th row of an unoccupied theater, with a 3° angled floor and a constant 5 m ceiling height.

For this purpose, all the PARDOS capabilities will be available at the student's service. They will be able to make a range of adjustments: the floor and ceiling optimal angles; the impedances and densities of the materials in order to reduce the diffraction and reflection phenomena; to insonify theater areas with the Map Sound Module (Figs. 33 and 34) and; to simulate the expected audio response at any location with the Auralization Module. In this respect, students will be able to load a.wav file with different pure tones (e.g. 500 Hz, 1,000 Hz) to obtain the simulated audio that will be listened to by the theater attendees.

Finally, the students will be encouraged to accurately predict, check and mitigate the well-studied phenomenon known as 'seat dip effect', which consists in the sound attenuation that appears at low frequencies due to the periodical location of the seats. The effect typically varies from 80 to 300 Hz, and it will depend on the row spacing and height of the seats [36], [37].

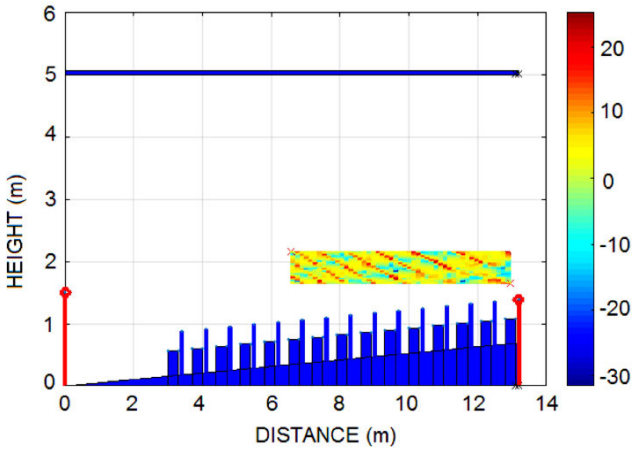

FIGURE 33. Sound Insertion Loss map simulation for parameters of Fig. 32.

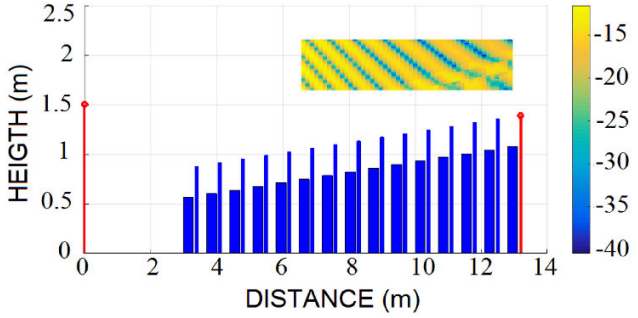

FIGURE 34. Sound Attenuation level map simulation for parameters of Fig. 32.

For such purpose, the scenario shown in Fig. 35 (where the seat spacing detail can be observed) will be created (e.g. with source, two edges and receiver). The frequency of the mentioned effect will be identified by reviewing the spectrum attenuation, and a parametric study to check both the influence of the variation of the height and spacing around the defined values and the effect of the material of the seats (densities and impedances of the edges) will be undertaken.

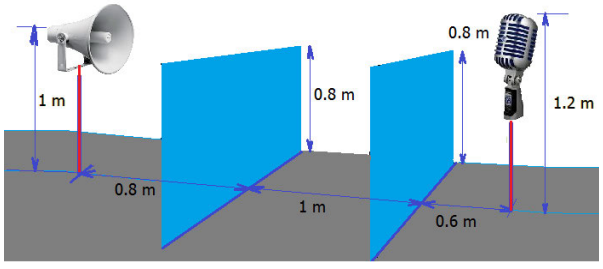

FIGURE 35. Seat spacing and height detail for the theater.

E. LEARNING RESULTS

With the practice exercises proposed, the students will be able to:

1. Reinforce their knowledge about Acoustics and different sound propagation phenomena, in a natural and easy way, by developing the mentioned Competences 1 and 2 throughout the 4 practices.
2. Analyze, design, and find solutions for real-scenario acoustic problems before they can arise, which will be performed in the practices where Competences 3, 4 and 6 are covered.
3. Be aware of the influence of obstacles of sound propagation-which could remain concealed without the proper simulations- by means of the reinforcing of Competences 3, 4 and 5.
4. Discern whether the desired SPL or any other acoustic requirement is met or not, this way addressing Competences 4 and 5.

IV. CONCLUSION

In this work, we have presented PARDOS as an intuitive educational tool applicable for allowing students to become familiar with Acoustics and to strengthen their knowledge about sound propagation mechanisms, such as diffraction and reflection. With PARDOS, the acoustic response (attenuation, IL, auralization analysis, etc.) can be estimated at any location within a wide variety of scenarios and acoustic sources, either predefined in the tool or created by the users.

Moreover, PARDOS incorporates a set of four guided practice exercises to allow students to acquire knowledge related to acoustic propagation phenomena, to design, optimize and tune scenarios, and to fulfill the desired acoustic requirements. In addition, since PARDOS is based on MATLAB, with a user-friendly GUI, it also allows access to all the potential post-processing capabilities embedded in MATLAB for any of the results obtained by the tool.

Unlike existing professional tools, which require high computing times and demand extensive training, PARDOS can be used almost immediately by students with no prior notions of acoustics. They can develop skills in designing, simulating, and analyzing many real scenarios accurately, from a practical perspective and in a very short time, which form a key part of the tasks in the field of acoustics.

In conclusion, due to the advantages of the presented educational tool against professional software, PARDOS represents an excellent option for enhancing and improving student learning regarding sound propagation in any course related to Acoustics.

REFERENCES

[1] L. Savioja and U. P. Svensson, "Overview of geometrical room acoustic modeling techniques," *J. Acoust. Soc. Amer.*, vol. 138, no. 2, pp. 708–730, Aug. 2015, doi: 10.1121/1.4926438.

[2] E. Lakka, A. Malamos, K. G. Pavlakis, and J. A. Ware, "Spatial sound rendering—A survey," *Int. J. Interact. Multimedia Artif. Intell.*, vol. 5, no. 3, p. 33, 2018, doi: 10.9781/ijimai.2018.06.001.

[3] F. Mechel, "Improved mirror source method in roomacoustics," *J. Sound Vib.*, vol. 256, no. 5, pp. 873–940, 2002.

[4] M. Taylor, A. Chandak, Q. Mo, C. Lauterbach, C. Schissler, and D. Manocha, "Guided multiview ray tracing for fast auralization," *IEEE Trans. Vis. Comput. Graphics*, vol. 18, no. 11, pp. 1797–1810, Nov. 2012.

[5] C. Lauterbach, A. Chandak, and D. Manocha, "Interactive sound propagation in dynamic scenes using frustum tracing," in *Proc. IEEE Vis.*, Sacramento, CA, USA, Nov. 2007, pp. 1672–1679.

[6] G. I. Koutsouris, J. Brunskog, C.-H. Jeong, and F. Jacobsen, "Combination of acoustical radiosity and the image source method," *J. Acoust. Soc. Amer.*, vol. 133, no. 6, pp. 3963–3974, Jun. 2013.

[7] S. Siltanen, T. Lokki, S. Kiminki, and L. Savioja, "The room acoustic rendering equation," *J. Acoust. Soc. Amer.*, vol. 122, no. 3, pp. 1624–1635, Sep. 2007.

[8] L. Savioja, T. Lokki, and J. Huopaniemi, "Auralization applying the parametric room acoustic modeling technique-the div auralization system," in *Proc. Int. Conf. Comput. Auditory Display*, Kyoto, Japan, Jul 2002, pp. 219–224.

[9] F. Ihlenburg, *Finite Element Analysis of Acoustic Scattering*. New York, NY, USA: Springer, 1998.

[10] T. W. Wu, *Boundary Element Acoustics: Fundamentals And Computer Codes*. Southampton, U.K.: WIT Press, 2000.

[11] (Jul. 5, 2011). *CATT-Acoustic V9.1 by TUCT V2, V9*. Accessed: Aug. 18, 2020. [Online]. Available: http://www.catt.se

[12] (2018). *EASE—Enhanced Acoustic Simulator for Engineers. V4.4*. Accessed: Aug. 18, 2020. [Online]. Available: https://ease.afmg.eu/

[13] A. Gołaś and K. Suder-Dębska, "Analysis of dome home hall theatre acoustic field," *Arch. Acoust.*, vol. 34, no. 3, pp. 273–293, 2009.

[14] *COMSOL Acoustics Module*. Accessed: Aug. 18, 2020. [Online]. Available: https://www.comsol.com/acoustics-module#simulation-apps

[15] *ODEON Room Acoustics Software*. Accessed: Aug. 18, 2020. [Online]. Available: https://odeon.dk/.ODEONroomacousticssoftwarev.16

[16] J. H. Rindel, G. B. Nielsen, and C. L. Christensen, "Diffraction around corners and over wide barriers in room acoustic simulations," in *Proc. 16th Int. Congr. Sound Vib.*, Krakow, Poland, 2009, pp. 1–9.

[17] N. Tsingos, S. Lefebvre, C. Dachsbacher, and M. Dellepiane, "Extending geometrical acoustics to highly detailed architectural environments," in *Proc. 19th Int. Congr. Acoust. (ICA)*, Madrid, Spain, 2007, pp. 1–7.

[18] D. Schröder, "Physically based real-time auralization of interactive virtual environments," Ph.D. dissertation, Inst. Tech. Acoust., RWTH Aachen Univ., Aachen, Germany, 2011.

[19] T. Wendt, S. van de Par, and S. Ewert, "A computationally-efficient and perceptually-plausible algorithm for binaural room impulse response simulation," *J. Audio Eng. Soc.*, vol. 62, no. 11, pp. 748–766, Dec. 2014.

[20] J. C. Boscher, "BRASS - Brazilian Room Acoustic Simulator," XXVIII Encontro da Sociedade Brasileira de Acústica, Universidade Federal do Rio de Janeiro, Rio de Janeiro, Brazil, Tech. Rep. NBR 12179, 2018, doi: 10.17648/sobrac-87152.

[21] *MATLAB. Version 8.5.0, R2015a*, MathWorks, Natick, MA, USA, 2015. Accessed: Aug. 18, 2020.

[22] D. Pardo-Quiles and J.-V. Rodríguez, "A fast UTD-based method for the analysis of multiple acoustic diffraction over a series of obstacles with arbitrary modeling, height and spacing," *Symmetry*, vol. 12, no. 654, pp. 1–24, 2020.

[23] F. Michel, "Simulation and visualization of in-and outdoor sound," Ph.D. dissertation, Dept. Comput. Sci., Kaiserlautern Technical University, Kaiserslautern, Germany, 2008.

[24] F. Brinkmann, L. Aspöck, D. Ackermann, S. Lepa, M. Vorländer, and S. Weinzierl, "A round robin on room acoustical simulation and auralization," *J. Acoust. Soc. Amer.*, vol. 145, no. 4, pp. 2746–2760, Apr. 2019, doi: 10.1121/1.5096178.

[25] I. Rees, "Common pitfalls in computer modelling of room acoustics," Adrian James Acoust. Ltd., Proc. Inst. Acoust., Norwich, U.K., Tech. Rep. vol. 38. Pt. 1, 2016.

[26] J. B. Keller, "Geometrical theory of diffraction," *J. Opt. Soc. Amer.*, vol. 52, no. 2, pp. 116–130, 1962.

[27] R. G. Kouyoumjian and P. H. Pathak, "A uniform geometrical theory of diffraction for an edge in a perfectly conducting surface," *Proc. IEEE*, vol. 62, no. 11, pp. 1448–1461, Nov. 1974.

[28] A. D. Pierce, "Diffraction of sound around corners and over wide barriers," *J. Acoust. Soc. Amer.*, vol. 55, no. 5, pp. 941–955, May 1974.

[29] H. Min and X. Qiu, "Multiple acoustic diffraction around rigid parallel wide barriers," *J. Acoust. Soc. Amer.*, vol. 126, no. 1, pp. 179–186, Jul. 2009.

[30] K. Rasmussen, "Calculation methods for the physical properties of air used in the calibration of microphones," Dept. Acoustic Technol., Tech. Univ. Denmark, Lyngby, Denmark, Tech. Rep. PL-11b, 1997.

[31] D. A. McNamara, J. A. G. Malherbe, and C. W. I. Pistorius, *Introduction to the Uniform Geometrical Theory of Diffraction*. Norwood, MA, USA: Artech House, 1990.
[32] G. Koutitas and C. Tzaras, "A UTD solution for multiple rounded surfaces," *IEEE Trans. Antennas Propag.*, vol. 54, no. 4, pp. 1277–1283, Apr. 2006, doi: 10.1109/TAP.2006.872675.
[33] J.-V. Rodriguez, J.-M. Molina-Garcia-Pardo, and L. Juan-Llacer, "A hybrid UTD-PO solution for multiple-cylinder diffraction analysis assuming spherical-wave incidence," *IEEE Trans. Antennas Propag.*, vol. 56, no. 9, pp. 3078–3081, Sep. 2008.
[34] L. E. Kinsler, A. R. Frey, A. B. Coppens, and J. V. Sanders, *Fundamentals of Acoustics*. Hoboken, NJ, USA: Wiley, Dec. 1999.
[35] F. Fahy, and T. D. Rossing, *Foundations of Engineering Acoustics*. London, U.K.: Academic, 2001.
[36] K. Ishida, "Investigation of the fundamental mechanism of the seat-dip effect. Using measurements on a parallel barrier scale-model.," *J. Acoust. Soc. Jpn., E*, vol. 16, no. 2, pp. 105–114, 1995.
[37] P. Economou and P. Charalampous, "Seat dip effect using wave based geometrical acoustics (WBGA)," in *Proc. 23rd ICSV Conf.*, Athens, Greece, vol. 4, 2016, pp. 2970–2977.

DOMINGO PARDO-QUILES was born in Albox (Almería), Spain, in 1974. He received the degree in telecommunications engineering from the Universidad Politécnica de Valencia (UPV), Spain, in 1998. He was the Research Proficiency from the Universidad Politécnica de Cartagena (UPCT), in 2006. From 1999 to 2000, he has been an Ericsson Engineer involved in the roll out of cell networks in Spain. Since 2000, he has belonged to Navantia Cartagena Shipyard, where he is a responsible of Sonar Systems. He is currently a Lecturer with the Information Technologies and Communications Department (TIC), UPCT. His research interests include acoustic propagation models, underwater sensors, and radiowave propagation.

JOSÉ-VÍCTOR RODRÍGUEZ was born in Murcia, Spain, in 1975. He received the degree in telecommunications engineering from the Universidad Politécnica de Valencia (UPV), Spain, in 2001, and the Ph.D. degree in communications engineering from the Universidad Politécnica de Cartagena (UPCT), Spain, in 2006. Before his Ph.D. degree, he did his Master's Thesis at the Lund Institute of Technology, Lund University, Sweden. In 2002, he joined the Department of Information Technologies and Communications, UPCT, where he is currently an Associate Professor. His research interests include the modeling of radio wave propagation, the development of acoustic propagation models, and the obtaining of biomedical algorithms through biosensors.

IGNACIO RODRÍGUEZ-RODRÍGUEZ was born in Murcia, Spain, in 1980. He received the degree in industrial engineering from the Universidad Politécnica de Cartagena, Spain, in 2007, the M.Sc. degree in chemical engineering from the Universidad de Murcia, Spain, in 2014, the M.A. degree in gender equality from the Universitat Jaume I de Castellón, Spain, in 2018, and the Ph.D. degree in computer sciences from the Universidad de Murcia in 2020. He is currently pursuing the Ph.D. degree in gender studies with the Universitat d'Alacant, Spain. He is also a Researcher with the ATIC Research Group, Departamento de Ingeniería de Comunicaciones, Universidad de Málaga, Spain. His research interests include machine learning, e-health, gender issues, and information and communication technologies applied to social sciences.